

RUNX2 prompts triple negative breast cancer drug resistance through TGF- β pathway regulating breast cancer stem cells

Fengxu Lv^{a,1}, Wentao Si^{a,1}, Xiaodan Xu^b, Xiaogang He^c, Ying Wang^a, Yetian Li^{d,*}, Feifei Li^{a,*}

^a Department of Pathophysiology, School of Basic Medical Sciences, Anhui Medical University, Hefei, 230032, PR China.

^b Department of Pathology, The First Affiliated Hospital of Anhui Medical University, Hefei, 230022, PR China

^c Medical Faculty Mannheim, University of Heidelberg, Mannheim, 68169, Germany

^d Department of Orthopedics, The First Affiliated Hospital of Anhui Medical University, Hefei, 230022, PR China

ARTICLE INFO

Keywords:

Triple negative breast cancer
Chemoresistance
Cancer stem cells
RUNX2
TGF- β

ABSTRACT

Triple-negative breast cancer (TNBC) stands out as the most aggressive subtype within the spectrum of breast cancer. The current clinical guidelines propose treatment strategies involving cytotoxic agents like epirubicin or paclitaxel. However, the emergence of acquired resistance frequently precipitates secondary tumor recurrence or the spread of metastasis. In recent times, significant attention has been directed toward the transcription factor RUNX2, due to its pivotal role in both tumorigenesis and the progression of cancer. Previous researches suggest that RUNX2 might be intricately linked to the development of resistance against chemotherapy, with its mechanism of action possibly intertwined with the signaling of TGF- β . Nevertheless, the precise interplay between their effects and the exact molecular mechanisms underpinning chemoresistance in TNBC remain elusive. Therefore, we have taken a multifaceted approach from in vitro and in vivo experiments to validate the relationship between RUNX2 and TGF- β and to search for their pathogenic mechanisms in chemoresistance. In conclusion, we found that RUNX2 affects chemoresistance by regulating cancer cell stemness through direct binding to TGF- β , and that TGF- β dually regulates RUNX2 expression. The important finding will provide a new reference for clinical reversal of the development of chemoresistance in breast cancer.

Introduction

Breast cancer is one of the most common malignant tumors in women, profoundly impacting women's quality of life and health [1]. Among highly heterogeneous breast cancers, triple negative breast cancer (TNBC), which is negative for estrogen receptor, progesterone receptor, and HER-2, is considered to be the most dangerous among all types of breast cancers, and predominantly affects young female patients [2,3]. Since TNBC lacks a clear therapeutic target and there is no clearly recommended targeted drug so far, chemotherapy is still the main treatment for TNBC, and clinical guidelines mostly recommend the use of cytotoxic drugs to kill cells, such as the anthracycline drug epirubicin or the paclitaxel [4]. However, more than 50 % of patients may experience tumor recurrence within 3 to 5 years after treatment, mainly due to acquired chemoresistance leading to secondary recurrence or metastasis [5]. Therefore, it is of great clinical significance to explore the resistance mechanism of TNBC to find the corresponding target to

reverse the chemoresistance of TNBC.

Many studies have shown that some residual tumor cells develop phenotypic changes in response to chemotherapeutic agents that lead to drug resistance, which is most commonly seen in epithelial mesenchymal transition (EMT) and cancer stem cell CSC-like stemness transition [6–8]. This process involves alterations in several signaling pathways. Among them, TGF- β related signaling pathways have attracted much attention [9,10]. In recent years, studies have shown that TGF- β plays an important role in the self-renewal and differentiation of CSCs, especially breast cancer stem cell (BCSCs), but its precise molecular regulation mechanism in chemoresistance is still unclear [11,12].

In our previous study, we uncovered that a transcription factor, RUNX2, also known as core-binding factor (cbf- α), is a molecule that is highly active in the development and differentiation of bone tissues and the development of various tumors, especially in breast cancer bone metastasis [13,14], and it also plays a regulatory role in chemoresistance in some tumors [15,16]. Rajnee Kanwal et al. found that RUNX2 is a key

* Corresponding author.

E-mail addresses: liyietian1984@163.com (Y. Li), Feifei.Li@ahmu.edu.cn (F. Li).

¹ Contributed equally.

factor in paclitaxel acute chemotherapy-stimulated prostate cancer cells with upregulated expression. Knockdown of RUNX2 expression in CD133+ prostate cancer cells resulted in a significant decrease in the expression of the stem cell-associated marker CD44 and changes in BMP2 expression in the TGF- β superfamily. Knockdown of RUNX2 reversed chemoresistance to doxorubicin in a subset of CD133+ prostate cancer stem cells [17]. These suggest that RUNX2 might have a similar role in TNBC chemoresistance and that its mechanism of action may be related to TGF- β , however, relevant reports are not available.

Consequently, our research investigated into comprehending the roles played by TGF- β and RUNX2 in both stemness and chemoresistance within triple-negative breast cancer cells. We pursued such investigation through an array of in vivo and in vitro analyses, meticulously exploring the interconnected mechanisms. Of noteworthy significance, our ChIP experiments revealed the direct binding of RUNX2 to specific motifs within the promoter region of TGF- β , thereby exerting control over its expression. Intriguingly, our findings also unveiled the dual influence of TGF- β on RUNX2. In summary, our study elucidates the intricate workings of the RUNX2-TGF- β axis in the context of chemoresistance in triple-negative breast cancer. Moreover, our insights offer a fresh perspective on the realms of metastasis and chemoresistance within this specific subtype of breast cancer.

Materials and methods

Cell culture

MB-231 and SUM-149 were obtained from the American Type Culture Collection (ATCC, USA), and MDA-MB231 was maintained in high-glucose DMEM medium (PM150210, Procell) supplemented with 10 % fetal bovine serum (164210, Procell) and 1 % penicillin and streptomycin (PB180120, Procell). SUM-149 was cultured in Ham's F12 medium (L410KJ, BasalMedia) supplemented with 5 % fetal bovine serum, 5 μ g/ml of insulin (UNITED LABORATORIES), and 1 μ g/ml of hydrocortisone (R011855, RHAWN). MB-231 epirubicin-resistant cell lines (MB-231/EPI) were established as previously described [18]. All cultures were maintained in a humidified 5 % CO₂ incubator (Thermo Fisher Scientific, Waltham, MA, USA) at 37°C. All cells were authenticated by short tandem repeat profiling and tested free from mycoplasma.

Reagents and antibodies

Anti-CD44 (559942, 1:500) and anti-CD24 (555428, 1:500) for Flow Cytometry were purchased from BD Bioscience (Dallas, Texas, USA). Anti-RUNX2 (12556, 1:1000), Vimentin (5741, 1:1000), N-Cadherin (13116S, 1:1000) for western blotting were purchased from Cell Signaling Technology (CST, USA). Anti-CD44 (AF6186, 1:500), Anti-RUNX2 (AF5186, 1:500), p-Smad2 (AF8314, 1:1000), Smad2/3 (AF6367, 1:500) and TGF- β (BF8012, 1:500) for western blotting were purchased from Affinity (Affinity Biosciences, USA). GAPDH (Servicebio, GB11002, 1:2000) and β -actin (Abcam, ab8226, 1:1000) were purchased for western blotting.

Cell transfection

MB-231/EPI cells were seeded in six-well plates and incubated for 24 h. Lentivirus containing shRNA (shRUNX2, NC; MOI=10) was added when cell reached 30-50 % confluency. Then, the supernatant was replaced with fresh medium after 24 h, followed with the observing the GFP fluorescence under a microscope at 72 h and stable line selection by puromycin addition (2 μ g/ml). MB-231/EPI cells with shRNA NC infection were used as a negative control. Similarly, the RUNX2 over-expression (denoted as RUNX2) and the negative control (denoted as Vector) SUM-149 cell lines were generated by utilizing the aforementioned lentiviral strategy.

RNA isolation and real-time quantitative polymerase chain reaction (qRT-PCR)

Total RNA was extracted using Trizol reagent (CWbio) according to the manufacturer's instructions. The concentration and quality of RNA were monitored using a NanoDrop one spectrophotometer (Thermo Fisher Scientific). An amount of 1 μ g of RNA was used to synthesize cDNA using the RT reagent Kit gDNA Eraser (E047, NovoScript). The corresponding cDNAs were subjected to quantitative PCR analysis using SYBR Green (AG11701-S) and relative RNA amount was calculated by $2^{-\Delta\Delta C_t}$ method with the normalization to β -actin. All primers were derived from Sangon Biotech (Shanghai). The relevant primers for qRT-PCR assays are listed in Supplementary Table S1.

Western blot

Total proteins were extracted with RIPA lysis buffer (biosharp) containing protease inhibitors (Thermo Fisher Scientific), and the protein concentrations were detected with BCA Protein Assay Kit (P0012, Beyotime). Sodium dodecyl sulfate-polyacrylamide gel electrophoresis (SDS-PAGE) was used to separate the proteins that were transferred afterward onto 0.45 μ m PVDF membranes (IPVH00010, Millipore). The membranes were blocked with 5 % non-fat milk for 2 h at room temperature and incubated overnight at 4°C with primary antibodies. Washed by TBST for three times, it would be followed by incubations with secondary antibodies. Finally, the protein bands were developed by using an enhanced chemiluminescence detection reagent (D045, Bridgen) and imaged by using an Image Lab (BIO-RAD). GAPDH and β -actin were selected to be the loading controls. Three independent experiments were conducted. Full-length original western blots in this article are provided in Supplementary File.

Cellular drug resistance method

Exponentially growing cells were seeded (1×10^4 cells/well) into the 96-well plates and incubated for 24 h at 37 °C with DMEM culture medium. Then the cells were cultured for 48 h at a range of concentrations of epirubicin. MTT reagent (KGA312, KeyGEN BioTECH, Jiangsu, China) were added to each well to assess the number of viable cells. The cells were incubated with MTT for 4 h, 150 μ l DMSO per well was added to dissolve the production of formazan. The absorbance of each well was assessed on a Multiskan™ FC reader at 490 nm. The definition of half maximal inhibitory concentration (IC₅₀) was the concentration of reagents needed to inhibit 50 % of cellular proliferating ability after 48 h treatment. The result of IC₅₀ was calculated using GraphPad Prism 7 software.

Migration and invasion assays

Cells preconditioned in DMEM basal medium (without 10 % FBS) for 12 h were placed into the upper chamber of the 24-well plate transwell insert (353097, Corning) at a density of 5×10^4 cells/well, and 600 μ l of DMEM medium containing 10 % FBS were added to the bottom chamber. After incubation in 37°C for 24 h (migration) or 48 h (invasion), the cells were fixed with 10 % formalin (YULU) for 30 min, following by staining with 0.1 % crystal violet (C8470, Solarbio) for 15 min. After wiping the non-migratory cells in the inner side of the upper chamber, images of migrated cells were captured from three randomly selected fields under the microscope, and the number of cells in each field was calculated. The invasion assay was similar to the migration assay, where the upper chamber was coated with matrix gel (356234, Corning).

Colony formation

In the colony formation assay, 1×10^3 treated cells were coated into

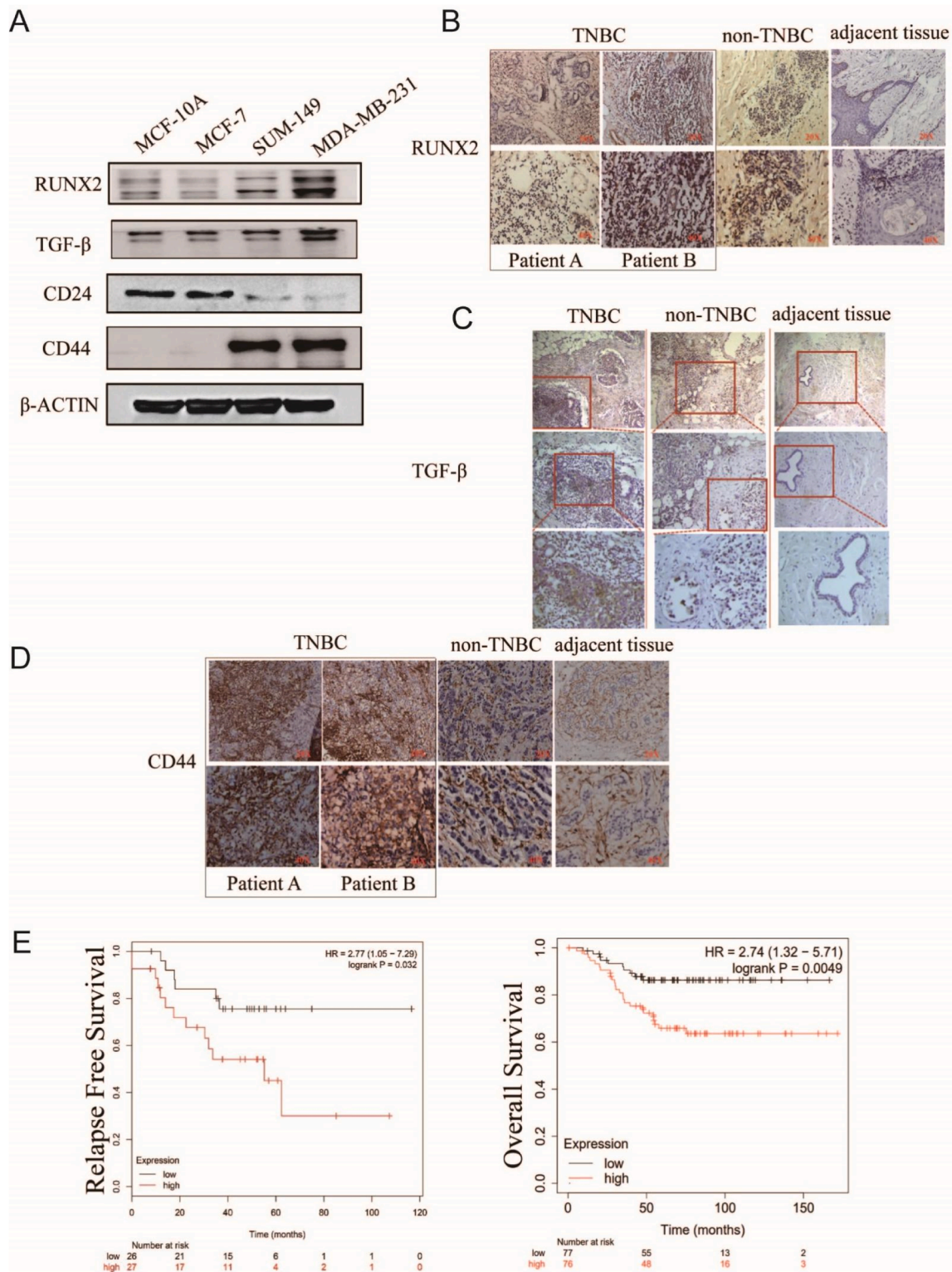


Fig. 1. RUNX2 and TGF-β are strongly associated with breast cancer malignancy.

6-well plates. In case of plate clones for resistance-related assays, the medium was changed to medium containing a certain concentration of Epi on the third day. After 10 days of incubation, the cells were washed twice with phosphate buffer solution (PBS), fixed with 4 % poly-methanol (BL539A, biosharp) for 10 min and stained with 0.1 % crystal violet solution at 10 min. Formed clones consisting of at least 50 cells were counted as a colony. The number of colonies was calculated using Image J software and the experiment was repeated three times.

Mammospheres assay

The protocol of Johnson et al. (2013) [11] was adapted in the following way. MB-231, MB-231/Epi cells were trypsinized and washed in PBS. 6-well attachment plates were coated with 0.7 % agarose gel to avoid cell adhesion. Nearly 1×10^4 cells per well were plated in the prepared 6-well flat-bottomed culture plates in DMEM/F12 (Gibco, NY, USA) supplemented with 10 ng/ml hr-bFGF (PeproTech, Rocky Hill, NJ)

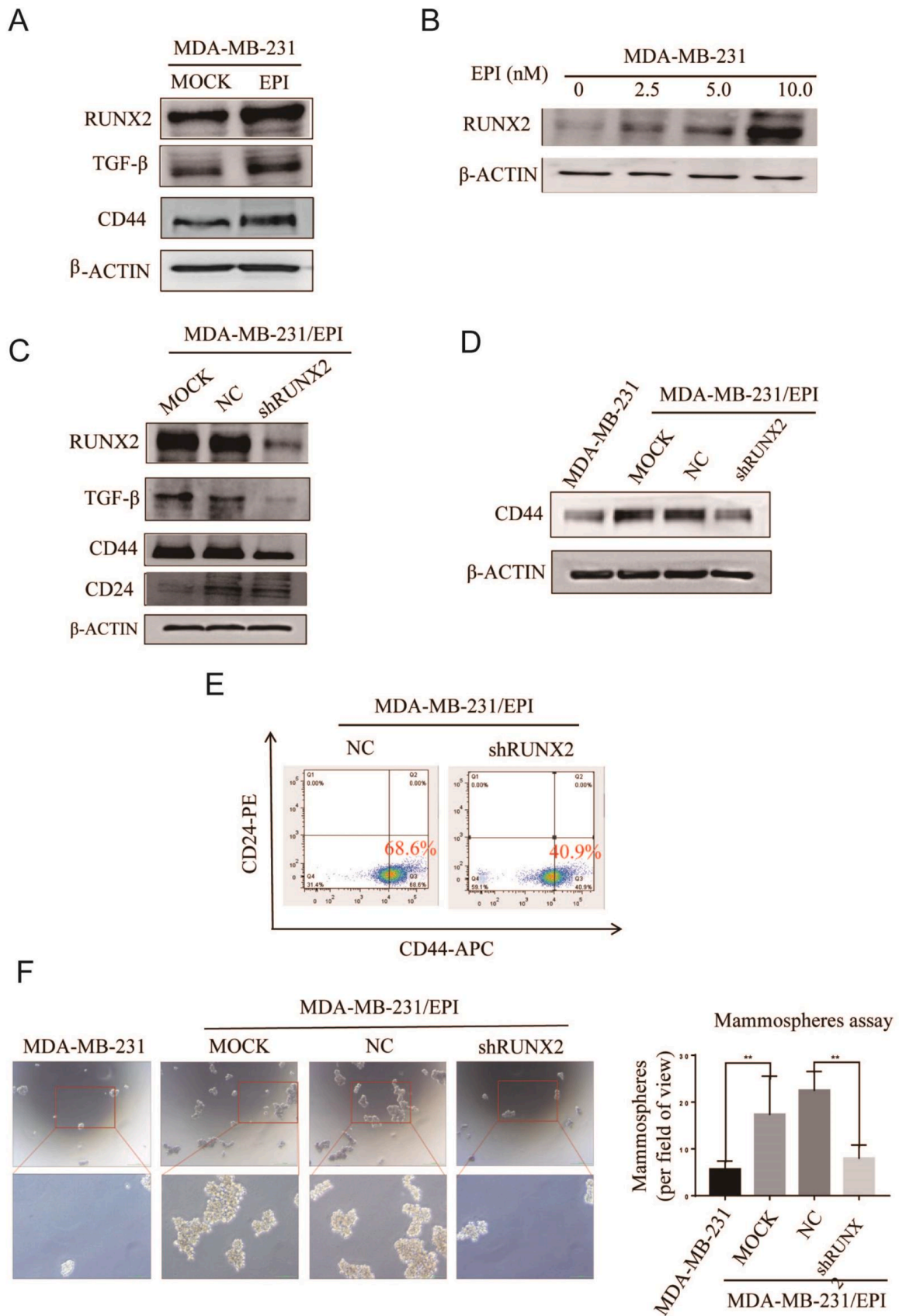


Fig. 2. Influence of RUNX2 on the stemness of drug-resistant cells in triple-negative breast cancer.

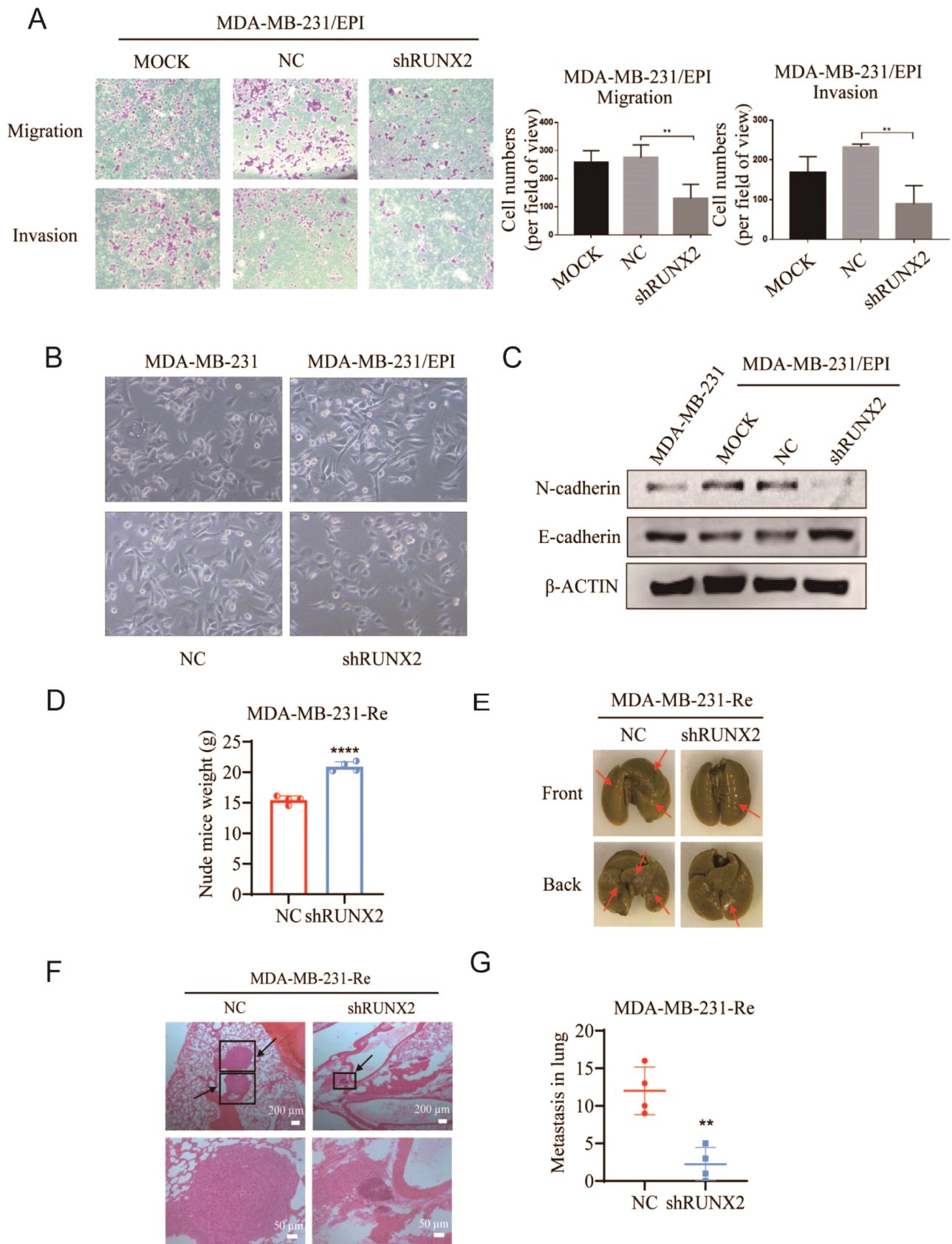


Fig. 3. Influence of RUNX2 on resistance and proliferation of drug-resistant breast cancer cells in triple-negative breast cancer.

and 20 ng/ml EGF (Thermo Fisher Scientific) and 1 × B27 (Gibco, NY, USA). After culturing for 5-8 days, spheres were photographed. Mammosphere-forming efficiency (MSFE) of spheres with the diameter greater than 50 μm was calculated.

Chromatin immunoprecipitation (ChIP) assay and data analysis

Cells were crosslinked with 37 % formaldehyde and lysed in SDS buffer. Then, the DNA was fragmented by using sonication. For RUNX2 binding sites on TGF-β promoter, ChIP assay was performed as we previously reported [19]. The eluted DNA fragments were turned to qRT-PCR assay, and the values generated from immunoprecipitated samples were normalized to those of the corresponding input samples. Besides, qRT-PCR products were stored at -20°C in a refrigerator until subsequent agarose gel electrophoresis (AGE). Primers sequences were shown in Supplementary Table S2.

Animal experiments

All animal experiments were approved by the Ethics Committee of Anhui Medical University. In the Subcutaneous xenograft experiments, Five-week-old male BALB/c nude mice were randomly divided into 4 groups (4 mice in each group), and MB-231/Epi-NC cells, MB-231/Epi-shRUNX2 cells (5 × 10⁶/0.1 ml PBS) were implanted into the armpit of each mouse, and one group each from the control and experimental groups was injected with 4mg/kg epirubicin via the intraperitoneal injection every three days. After 9 days, we began to use digital vernier calipers to measure the tumour size every three days, and tumour volume was calculated according to the following formula: volume = 1/2 × (width² × length).

In the lung metastasis experiments, Five-week-old nude mice were randomly divided into two groups (n = 4 in each group) and injected with 100 μl of MB-231/Epi-NC cells, and MB-231/Epi-shRUNX2 cells (1 × 10⁶) via the tail vein, respectively. Thirty days after cell injection, mice were euthanized and necropsied to assess metastatic burden. Lung tissues of mice were embedded in paraffin for hematoxylin and eosin (HE) staining.

Flow cytometry

Antibodies for flow cytometry analysis were purchased from BD Bioscience. For the flow cytometry analysis of surface markers, the cells were stained on ice with fluorescence-conjugated antibodies for 30 min according to the manufacturer's instructions. Stained cells were finally evaluated by flow cytometry and analyzed through FlowJo Software.

Immunohistochemistry (IHC) and quantification

FFPE (formalin-fixed, paraffin-embedded) sections acquired from patients or mice tissues were deparaffinated, dehydrated and subjected to antigen retrieval by placing them in citrate buffer in a 98°C water bath for 10 min to shelter endogenous peroxidase activity. The samples were also subjected to H₂O₂ treatment and blocked with 5 % BSA solution for 30 min. Thereafter, the samples were incubated with specific primary antibodies overnight at 4°C. On the following day, sections were incubated with corresponding secondary antibodies and then analyzed using a DAB staining kit (ZSGB-BIO).

Statistical analysis

All experiments were repeated at least three times. Student's t-test was used to analyze the differences between the two groups. All statistical analyses were performed with the GraphPad Prism (GraphPad Software) and SPSS 20.0 software as we described before [14]. Only when P < 0.05, the results would be considered with statistically significant differences. All data were presented as mean ± SD (n = 3

independent experiments). For all tests, p < 0.05 was considered significant (ns: not significant, *, P < 0.05; **, P < 0.01; ***, P < 0.001; ****, P < 0.0001).

Results

RUNX2 and TGF-β plays indispensable roles with triple-negative breast cancer

First, we examined the protein expression levels of RUNX2, TGF-β and the stem cell marker CD44 in normal breast epithelial cells MCF-10A, ER+ cells MCF-7, inflammation-associated TNBC cells SUM-149, and TNBC cells MB-231, and found that RUNX2, TGF-β, and CD44+/CD24- were higher in triple-negative breast cancer cells than in non-triple-negative breast cancer cells than in normal breast epithelial cells (Fig. 1A). Next, we examined the clinicopathologic specimens of TNBC, non-TNBC, and para-cancerous tissues by immunohistochemistry, and the results indicated that the expression levels of RUNX2 and TGF-β were significantly higher in pathologic specimens of triple-negative breast cancer compared with non-TNBC specimens and para-cancerous tissue samples (Fig. 1B-C). The differences in the expression of the breast cancer stem cell marker CD44 in patient tissue samples were basically consistent with the differences in the expression of RUNX2 and TGF-β in patient tissue samples (Fig. 1D). Based on the Kaplan-Meier Plotter database (<http://kmplot.com/analysis/index.php>), we found that TGF-β expression showed a positive correlation with overall survival and relapse-free survival of breast cancer patients (Fig. 1E). Taken together, our data demonstrated the positive correlation of TGF-β expression with poor prognosis in breast cancer.

RUNX2 mediated chemoresistance is associated with tumor cell stemness

First, we examined the expression of RUNX2, TGF-β and the stem cell marker CD44+/CD24- in the previously chronic induction-established triple-negative breast cancer-resistant cell line MB-231/EPI [18], and found that the expression of these proteins was increased in MB-231/EPI (Fig. 2A). Next, we selected appropriate lower concentration gradients of epirubicin to acutely stimulate MB-231 and SUM-149 cells, and detected the expression of RUNX2, TGF-β and the stem cell marker CD44+/CD24-, finding that the expression of RUNX2, TGF-β and CD44+/CD24- increased dose-dependently with the increase of epirubicin concentration to a certain extent (Fig. 2B, Fig. S1A). These results tentatively suggested that the stemness of drug-resistant cells was enhanced compared with that of parental cells and that the stemness was related to RUNX2 and TGF-β. To further investigate the relationship between RUNX2 and drug resistance, we established drug-resistant cells with knockdown and overexpression of RUNX2, and found that the expression of TGF-β and CD44+/CD24- were consistent with that of RUNX2 (Fig. 2C, Fig. S1B). Controversially, knockdown of RUNX2 expression reversed the expression of breast cancer stem cell marker proteins and TGF-β in drug-resistant cells (Fig. 2D). Flow assay results showed the same results (Fig. 2E). Microsphere assay results also showed that knockdown of RUNX2 expression in drug-resistant cells reversed the elevated stem cell microsphere-forming ability of drug-resistant cells relative to parental cells (Fig. 2F).

RUNX2-mediated alterations in tumor drug resistance involved in affecting the ability of tumors to colonize and metastasize

In order to investigate the effect of RUNX2 expression on TNBC drug resistance, MTT assay was performed to detect the drug resistance of the cells, and it was found that knockdown of RUNX2 expression reversed the increased chemotherapeutic resistance of MB-231/Epi cells compared to parental MB-231 cells, and the resistance index of the knocked-down cells to epirubicin was only 45.2 % of that of MB-231/Epi cells, and that to paclitaxel was only 34.26 % of that of MB-231/Epi cells

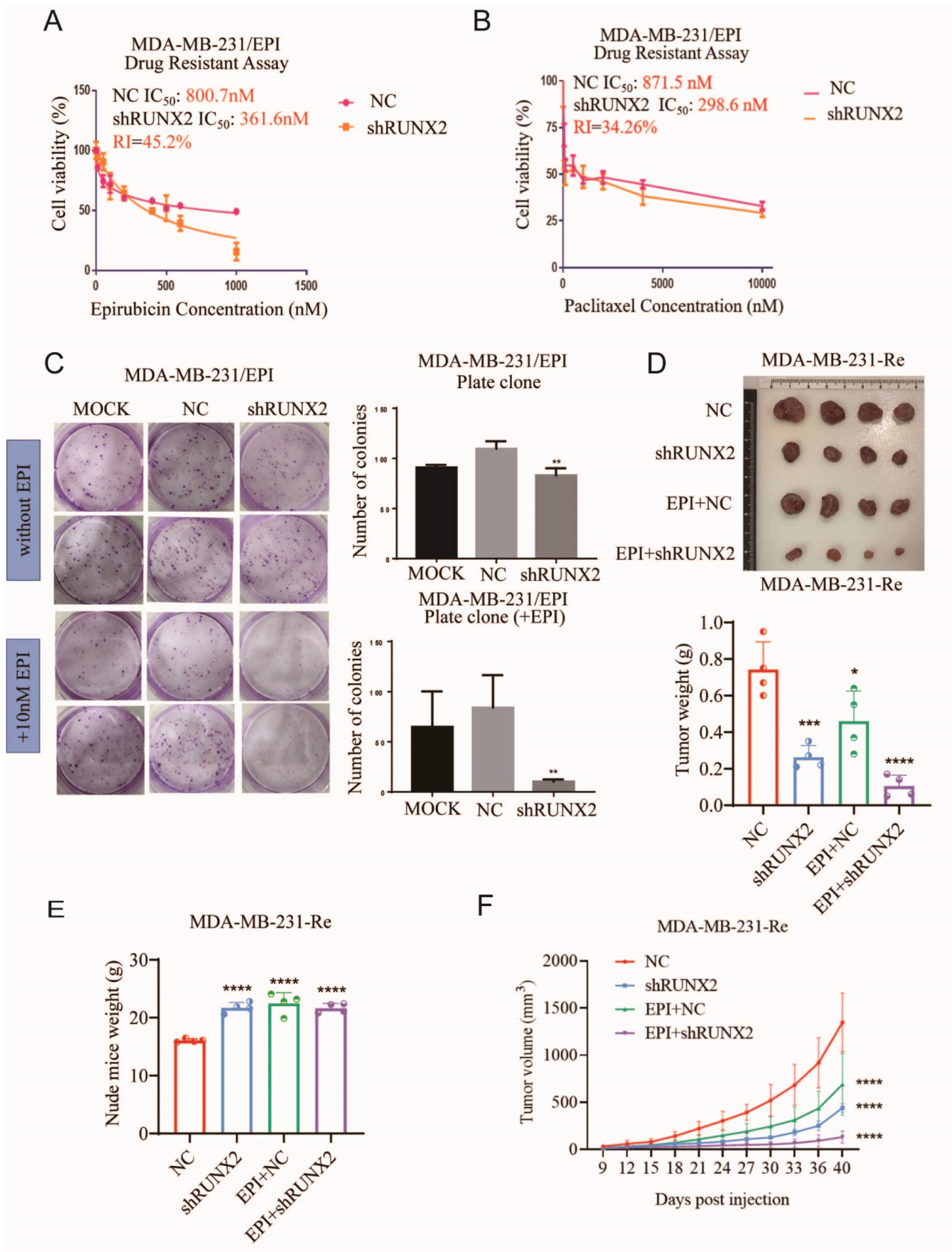


Fig. 4. The effect of shRUNX2 on the migration and invasion of drug-resistant cells in TNBC.

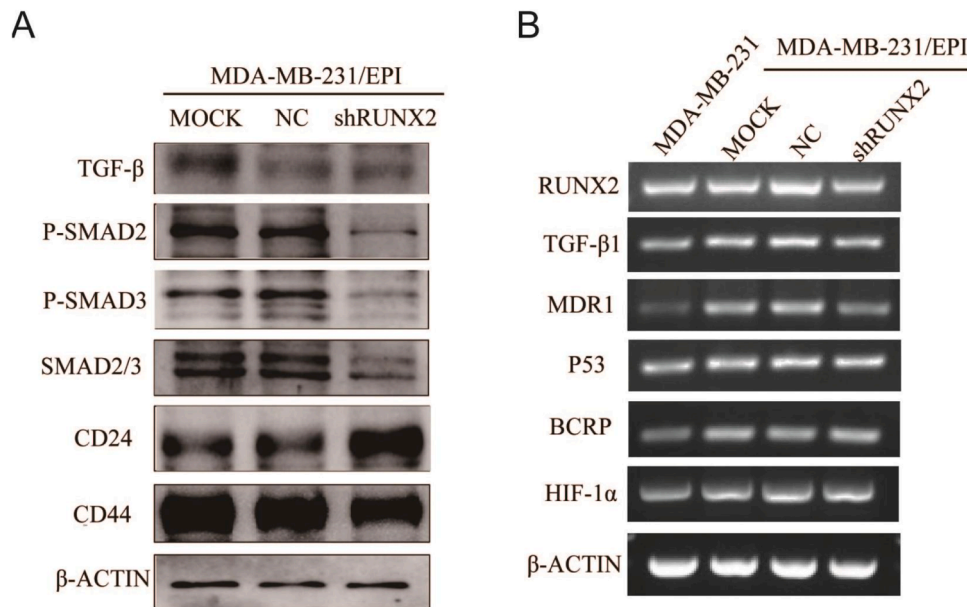


Fig. 5. Runx2 regulates TNBC chemoresistance by regulating TGF- β signaling pathway and transcription level expression of MDR1.

(Fig. 3A-B). The results of the plate cloning assay also showed that the clones formed by the cells after knockdown of RUNX2 expression in drug-resistant cells were slightly smaller in size and fewer in number (Fig. 3C). After the addition of medium containing 10 nM epirubicin to the clone culture, it was found that the clones formed by the MB-231/Epi cells and the negative control MB-231/Epi -NC cells were only slightly smaller than those formed without the addition of the drug, and their growth was almost unaffected, whereas the MB-231/Epi-shRUNX2 cells, in which the expression of RUNX2 was knocked down, were almost unable to grow and form clones during the addition of the drug (Fig. 3C). The same method also examined SUM-149 cells overexpressing RUNX2 but found opposite results (Fig. S1C-D). These results suggest that overexpression of RUNX2 increases the resistance of TNBC cell lines to epirubicin and promotes the development of chemotherapy resistance. The cells overexpressing RUNX2 were significantly more resistant to paclitaxel and epirubicin as shown in MTT assay, on one hand, indicate the presence of cross-resistance to chemotherapeutic drugs; on the other hand, suggest a potentially heightened role of RUNX2 in governing resistance to paclitaxel-based chemotherapy. Subsequently, tumorigenic experiments also confirmed that knocking down RUNX2 could reverse the tumor growth and proliferation caused by drug resistance (Fig. 3D-F). The above experimental results showed that the alteration of RUNX2 expression level affected the proliferation ability of drug-resistant cells. We continued to explore its effect on the metastatic ability immediately afterward. We confirmed that knockdown of RUNX2 reversed the increased migratory and invasive abilities of drug-resistant cells compared with parental cells, while overexpression of RUNX2 increased the migratory and invasive abilities of SUM-149 cells by Transwells (Fig. 4A, Fig. S2A). Knockdown of RUNX2 in drug-resistant cells resulted in characteristic mesenchymal cell morphology changes (Fig. 4B) and reversed the increase in the mesenchymal marker N-Cadherin and the decrease in the epithelial marker E-Cadherin in drug-resistant cells (Fig. 4C). To verify this phenomenon *in vivo*, we used an experimental metastasis mouse model in which nude mice were injected with intravenous MB-231/EPI and MB-231/EPI-shRUNX2, and it was observed through HE staining that the occurrence of lung metastasis was inhibited after knocking down RUNX2 compared with control mice (Fig. 4D-G).

RUNX2 modulates chemoresistance in triple-negative breast cancer by regulating the TGF- β signaling pathway and transcriptional expression of MDR1

As a result of our previous experiments, we have found that changes in the expression level of RUNX2 affect the expression of TGF- β (Fig. 2C). Therefore, we examined the changes in the expression of TGF- β pathway related markers in cells by immunoblotting assay, and found that knockdown of RUNX2 decreased the expression of TGF- β as well as phosphorylated p-Smad-2, p-Smad-3, and insignificant changes in the total proteins Smad2/3, whereas the changes in the stem cell markers were in agreement with the previous results, suggesting that the knockdown of RUNX2 reversed the effects of chemoresistance in relation to the TGF- β pathway (Fig. 5A). Next, we further explored whether RUNX2 regulates other resistance-related genes in addition to the TGF- β signaling pathway, which in turn affects TNBC chemoresistance. RT-PCR was performed to detect the expression of gene transcript levels of TGF- β 1, multidrug resistance protein MDR1, p53, BCRP, and hypoxia-inducible factor Hif-1 α in MB-231, MB-231/Epi, MB-231/Epi-NC, and MB-231/Epi-shRUNX2 cells. The results showed that MDR1, TGF- β 1, BCRP, Hif-1 α , p53 transcript levels were upregulated in MB-231/Epi relative to MB-231. In contrast, knockdown of RUNX2 expression in drug-resistant cells only reversed the transcript levels of TGF- β 1 and MDR1 (Fig. 5B). To a certain extent, this suggests that the reversal of drug resistance by knocking down RUNX2 may be through the regulation of the transcriptional expression levels of TGF- β 1 and MDR1, and has little relationship with other drug resistance-related genes. The RT-PCR results in SUM-149 with elevated RUNX2 expression further confirmed that the increased drug resistance by elevated RUNX2 expression was related to the regulation of TGF- β and MDR1 transcript expression levels by RUNX2 (Fig. S2B).

RUNX2 directly targets TGF- β to play an important role in chemoresistance in triple-negative breast cancer

To further explore the relationship between the effects of RUNX2 and TGF- β , we induced MB-231/Epi-shRUNX2 with a lower concentration of recombinant human TGF- β cytokine, and the results of microsphere formation assay, flow cytometry and plate cloning assay showed that TGF- β restored to a certain degree the diminished cell stemness caused by the knockdown of RUNX2 (Fig. 6A-C). Resistance to epirubicin was

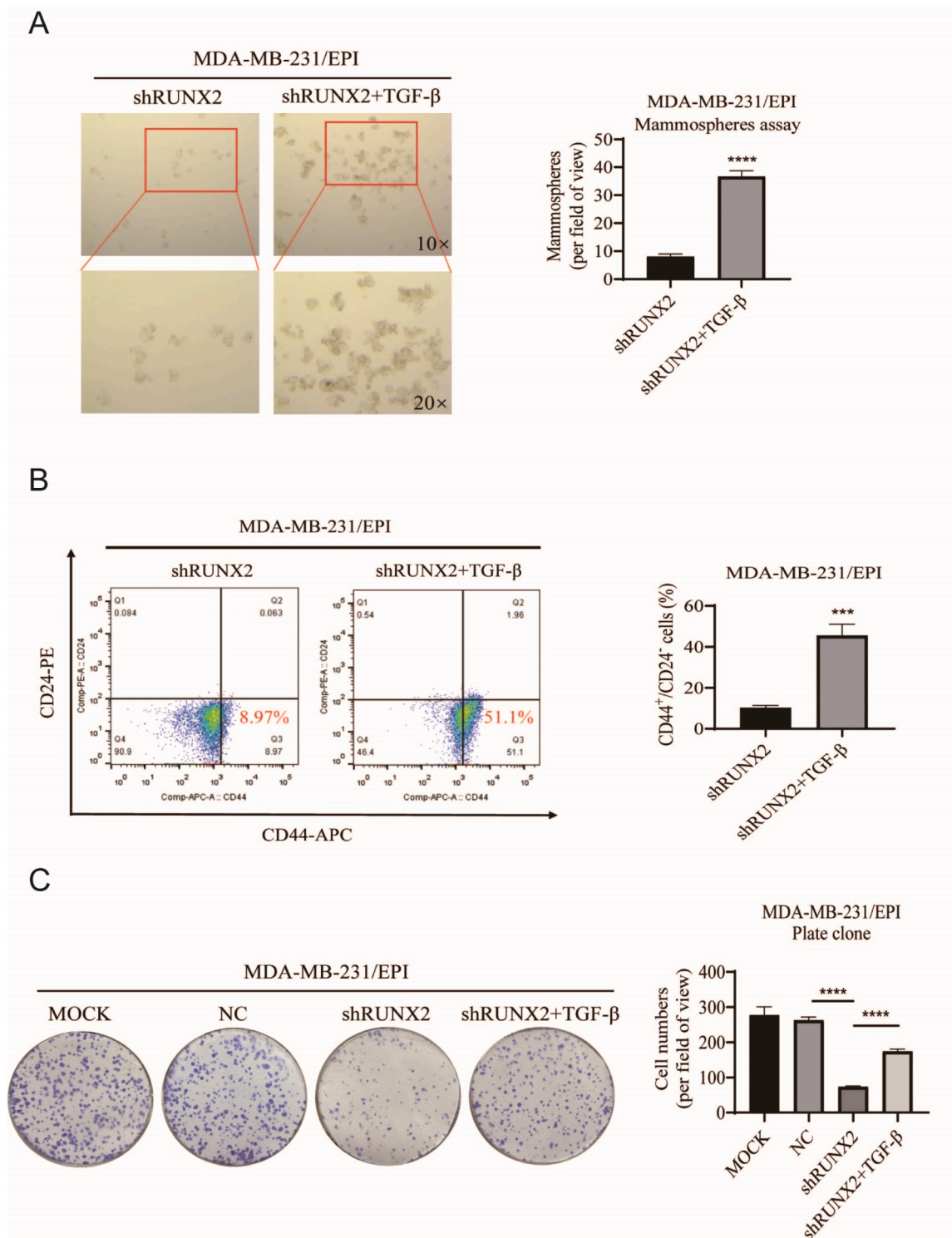


Fig. 6. TGF-β restores the effect of shRUNX2 on the stemness and metastatic ability of drug-resistant cells in TNBC.

also restored in the cells of the added TGF-β group as measured by MTT drug toxicity assay (Fig. 6D). Next, we found that TGF-β also restored the reduced cell metastatic ability caused by knockdown of RUNX2, as verified by observation of cell morphology and Transwell assay (Fig. 6E-F).

After initially verifying the potential regulatory relationship between RUNX2 and TGF-β, we speculated whether RUNX2 acts by directly activating TGF-β expression. Therefore, we predicted potential binding

sites for RUNX2 in the TGF-β promoter region based on the JASPAR database (<http://jaspar.genereg.net/>) (Table 1). Among the 11 candidate binding sites, the top 3 binding sites with the highest scores (sites 1, 2, and 3) were selected for further characterization. Subsequently, with the help of chromatin immunoprecipitation (ChIP) and qRT-PCR analyses as well as agarose gel electrophoresis, we found that all three sites were specifically enriched by RUNX2 in MDA-MB231/Epi cells with high levels of RUNX2 expression (Fig. 7A-B). Agarose gel

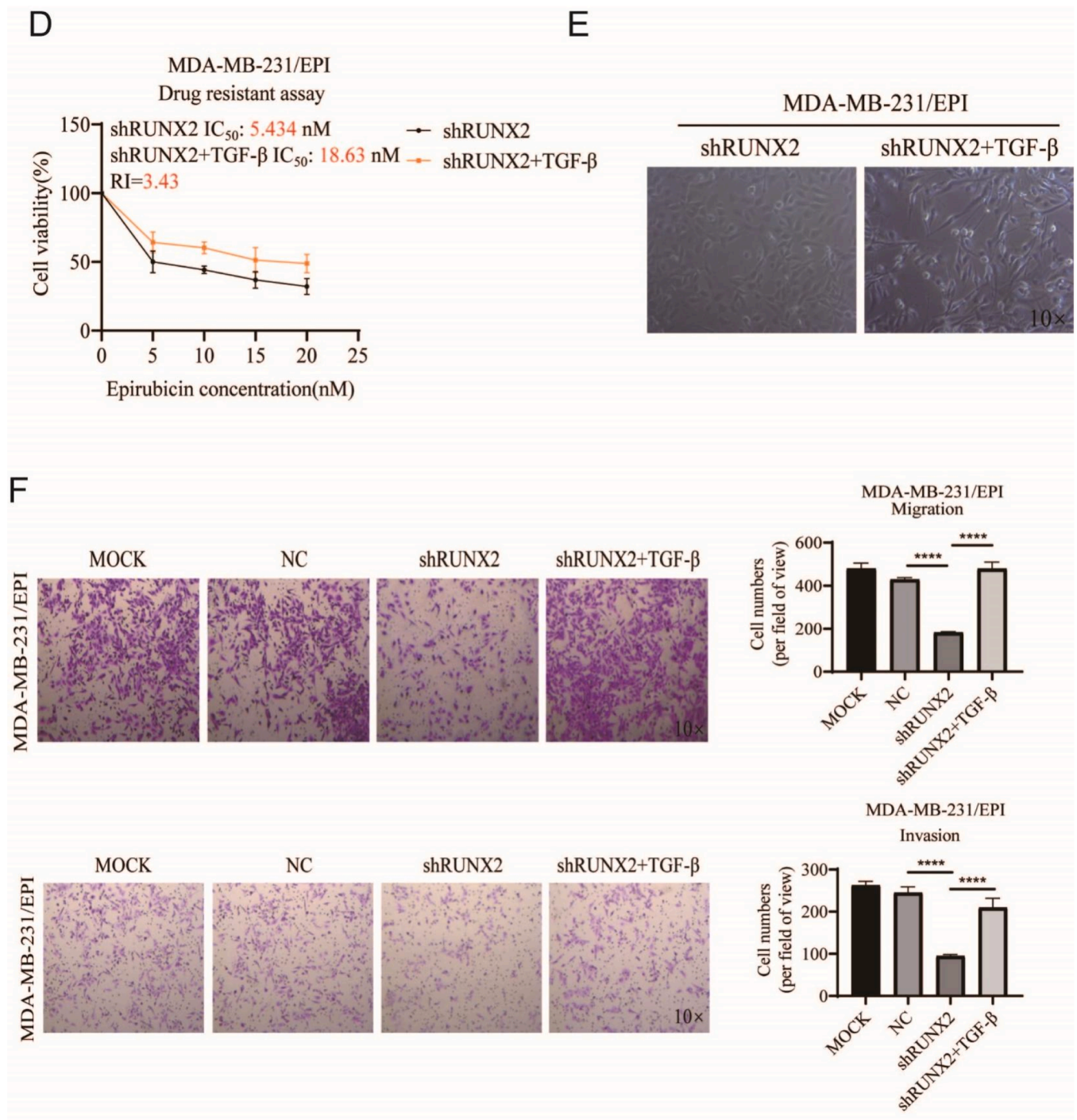


Fig. 6. (continued).

electrophoresis conclusively verified this (Fig. 7C). In summary, these data suggest that RUNX2 directly regulates TGF-β through specific binding motifs within the promoter region.

Regulation of RUNX2 expression by TGF-β is dual in triple-negative breast cancer

In order to examine whether TGF-β has an influence on the expression of RUNX2, we induced MB-231 with lower concentrations of recombinant human TGF-β cytokines (PeproTech, Rocky Hill, NJ) of 0 ng/ml, 2 ng/ml, 5 ng/ml, and 10 ng/ml for ten days, respectively, which was verified by western blot, and the results showed that the expression

of RUNX2 could be induced elevation (Fig. 8A). MTT drug toxicity assay also showed increased resistance to epirubicin in cells induced by 2 ng/ml TGF-β for ten days compared to cells induced by other concentrations (Fig. 8B). Use microsphere formation assay to detect cells, which were previously induced for ten days by 2 ng/ml TGF-β with higher RUNX2 expression revealed enhanced stemness of the cells, and consistent results were obtained by flow cytometry (Fig. 8C-D). Next, we further used a lower TGF-β induction concentration gradient of 0ng/ml, 0.5 ng/ml, 1 ng/ml, 1.5 ng/ml, 2 ng/ml, and increased the induction time to 15 days, and the immunoblotting results showed that the concentration of 1.5 ng/ml induced the best up-regulation of RUNX2 expression in MB-231 cells at the 15 days of induction (Fig. 8E). When the induction time

Table 1
 JASPAR analysis results for RUNX2 binding sites located within the promoter of TGF-β gene (Sequence ID:GRCh38:19:41355922:41353922).

Site	Score	Start	End	Strand	Predicted sequence
Site 1	11.202553	1735	1749	-	ATGCGCTGTGGCTTT
Site 2	7.346085	725	739	+	CTGCTGTGTGGGGAT
Site 3	6.6795735	813	827	+	TGGGCCTGGGGTCTC
Site 4	6.432458	1728	1736	+	CGCCCGCAA
Site 5	5.9454074	142	150	+	TTACCACCA
Site 6	5.881847	1242	1250	+	TCACCACCA
Site 7	5.7263823	1127	1135	+	CGACCGCTA
Site 8	5.7263823	1199	1207	+	CGACCGCTA
Site 9	5.1281776	933	941	-	GGACCACAC
Site 10	5.0655637	1724	1732	+	ACACCGCCC
Site 11	4.262197	818	826	-	AGACCCAG

was increased to 30 days, the concentration of 1ng/ml induced the most significant increase in RUNX2 expression (Fig. 8F). MTT drug toxicity assay also showed that the cells induced with 1.5ng/ml TGF-β for 15 days were more resistant to epirubicin than the parental MB231 cells, and the resistance index was 3.987 times higher than that of parental MB-231 cells (Fig. 8G). The MTT drug toxicity assay was performed on 0.5 ng/ml TGF-β-induced cells for 30 days, in which the expression of RUNX2 was not significantly up-regulated, and it was found that the cellular resistance was also little changed (Fig. 8H). All of the above experimental results indicated that TGF-β played a regulatory role on the expression of RUNX2, which further promoted cell stemness and drug resistance.

Discussion

With the advancement of diagnostic and treatment methods and

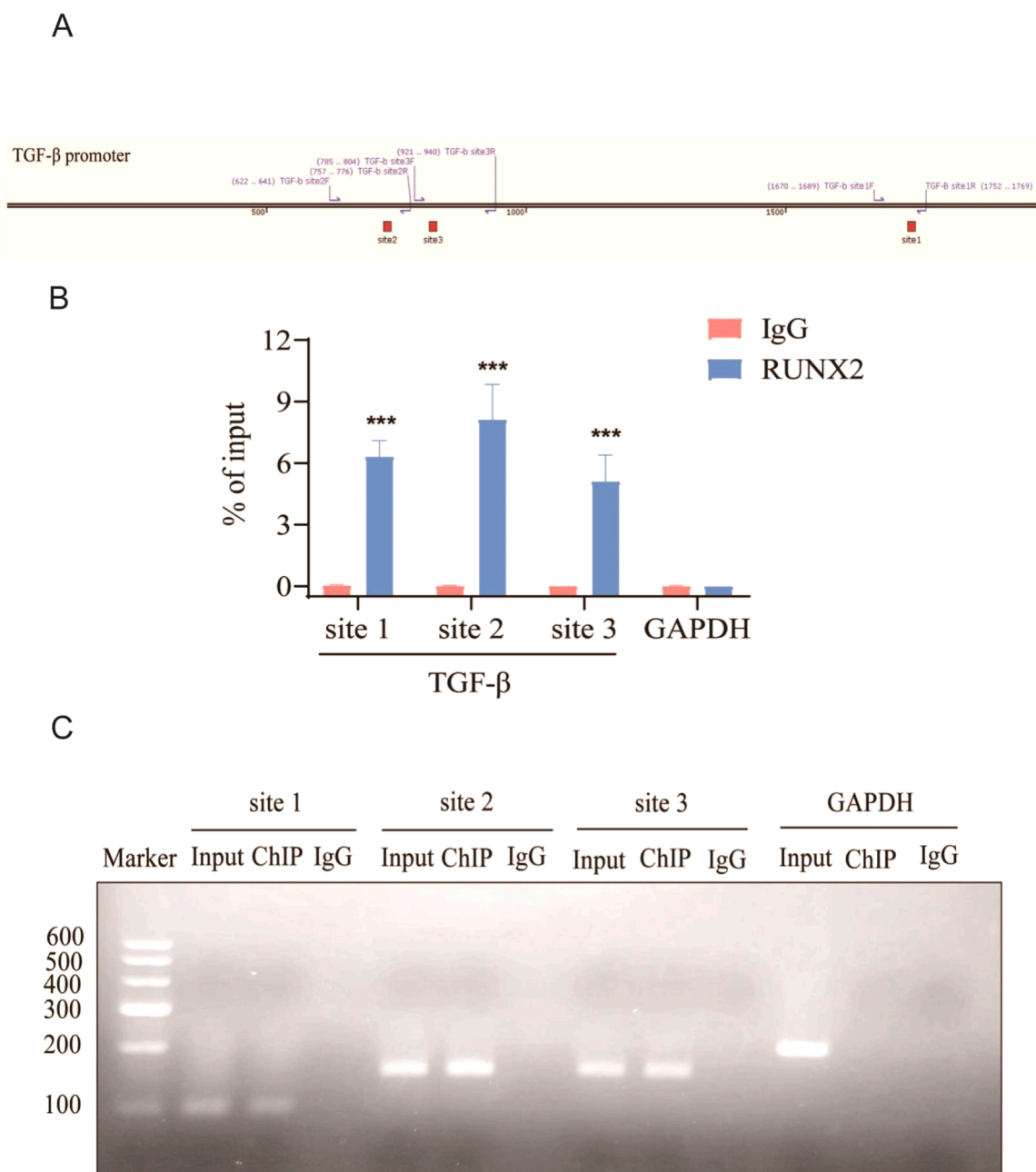


Fig. 7. RUNX2 binds directly to the TGF-β promoter region.

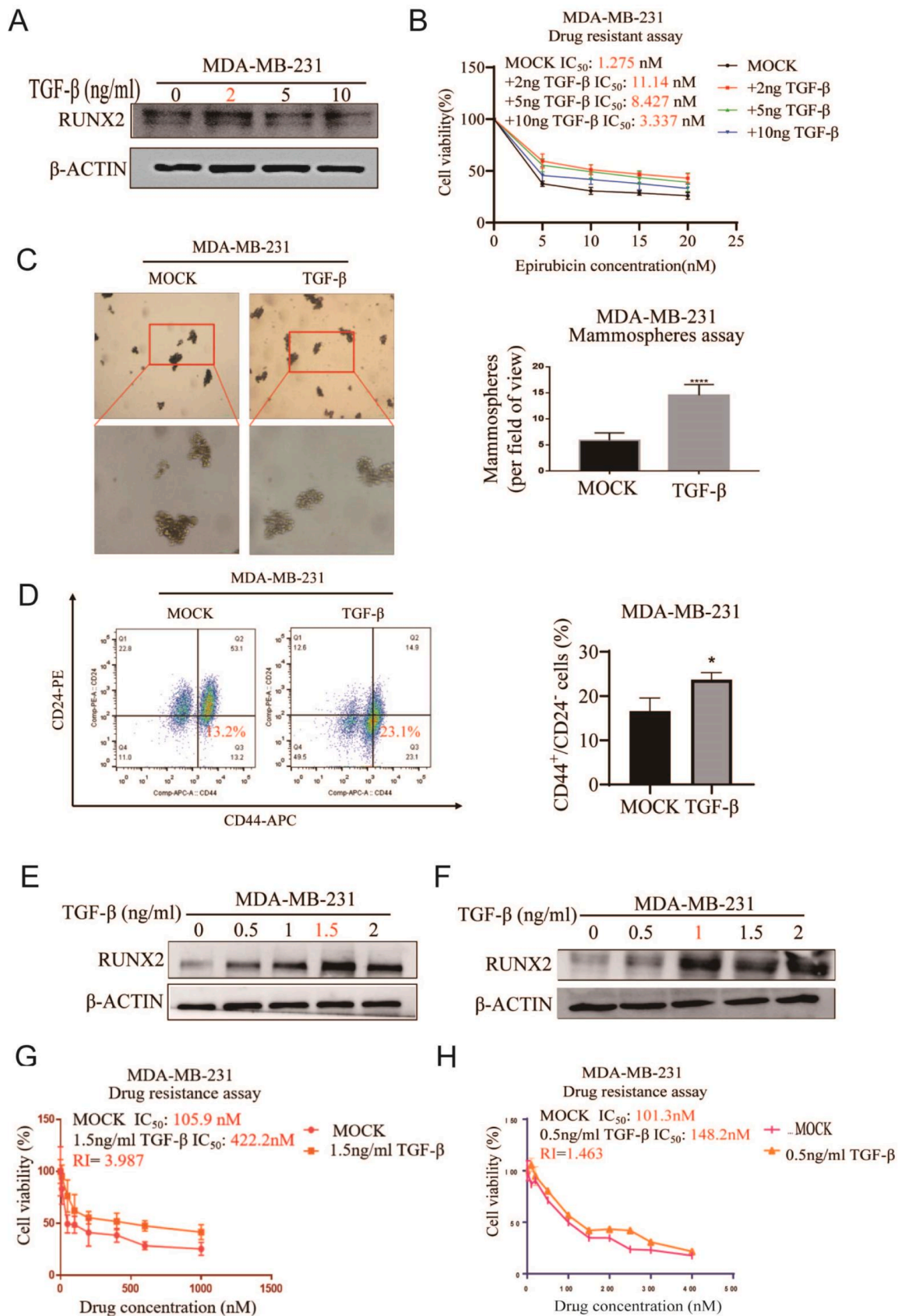


Fig. 8. TGF- β play a dual role in regulating the expression of Runx2 in TNBC cells.

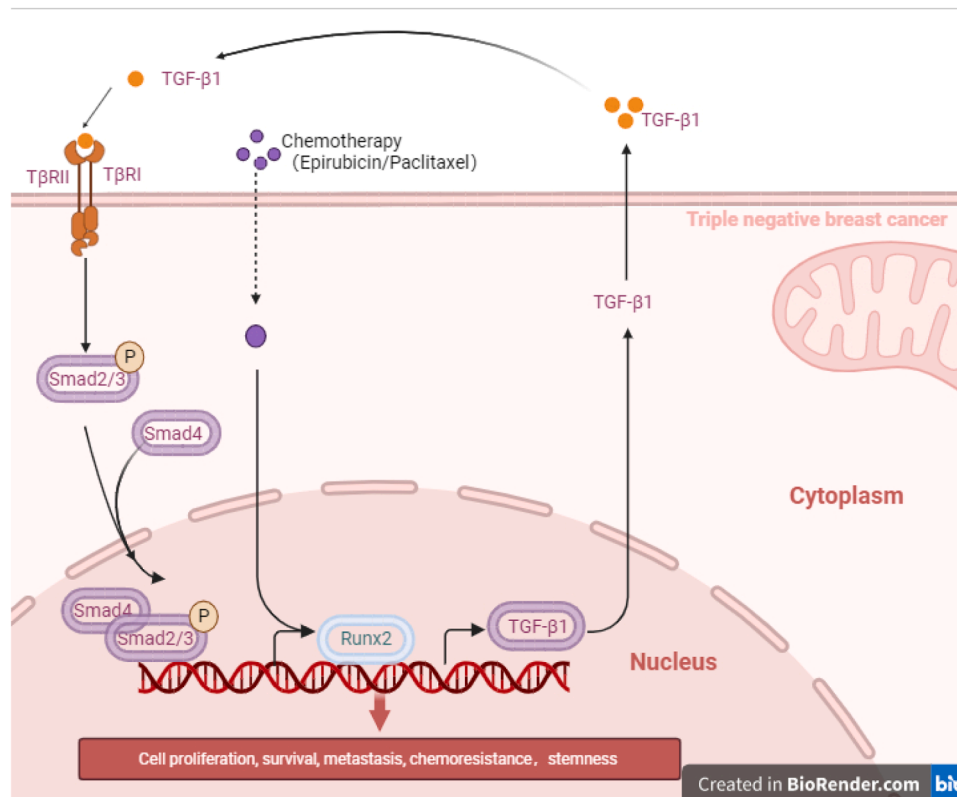


Fig. 9. A working model for the role of the RUNX2-TGF- β signaling axis in TNBC drug resistance.

increased awareness of breast cancer screening, the detection rate of breast cancer has increased while the mortality rate has decreased, with a five-year survival rate of up to 90 % after detection [20]. However, triple-negative breast cancer (TNBC) remains the major challenge in breast cancer treatment. In particular, the development of acquired chemoresistance is the major cause of tumor recurrence, metastasis and death in TNBC patients [21]. It is of great clinical significance to investigate the mechanism and prevent its development.

In recent years, the TGF- β -related signaling pathway, which often plays an important role as a key node in tumor progression, has also been demonstrated to be associated with chemoresistance induced by enrichment of tumor stem cells after chemotherapy in a variety of tumors [22–24], however, its specific mechanism remains unclear, especially in breast cancer. RUNX2, as a transcription factor that plays an important role in cancer development, has also shown to be closely related to chemotherapy resistance in colorectal cancer [25], prostate cancer [26] and pancreatic cancer [27], but the role and mechanism of anthracycline chemotherapy resistance in breast cancer have not been reported in detail.

Based on our preliminary findings on breast cancer stem cells and related malignant behaviors of breast cancer (e.g., invasion, metastasis, and tumorigenicity), we showed that RUNX2 has a direct regulatory function in them [28–30]. Thus, we confidently speculated that RUNX2 might play an equally important role in chemoresistance to such drugs, and that its specific mechanism might be closely related to TGF- β and tumor stem cell enrichment.

As expected, which is consistent with this, we constructed triple-negative breast cancer epirubicin resistant cells (MB-231/Epi) by acute stimulation and chronic induction, and verified that the expression of RUNX2 has a direct impact on the malignant behavior of drug-resistant breast cancer cells, and greatly influences the progression of chemoresistance. In vivo experiments, we used a variety of experimental means such as tail vein injection, subcutaneous injection, and intra-peritoneal injection, and similarly confirmed the role of RUNX2 in

triple-negative breast cancer. Importantly, in the current study, we demonstrated that RUNX2 has a definite regulatory effect on the TGF- β -related signaling pathway, and for the first time, we found that RUNX2 could directly target TGF- β by CHIP assay, which promotes the development of EMT and the increase in the proportion of CD44⁺/CD24⁻ highly invasive mesenchymal breast cancer stem cell subsets, thus leading to the chemoresistance of TNBC. Equally importantly, our experimental results suggest that TGF- β has a dual regulatory effect on RUNX2 expression, and the underlying mechanism may be related to the further promotion of RUNX2 expression and the enhancement of cancer cell resistance through autocrine effects. In conclusion, our data elucidate the synergistic mechanism of the RUNX2-TGF- β axis in triple-negative breast cancer cell stemness and chemoresistance, and provide a new therapeutic target for the development of clinically acquired chemoresistance (Fig. 9).

CRediT authorship contribution statement

Fengxu Lv: Data curation, Formal analysis, Methodology, Writing – original draft. **Wentao Si:** Formal analysis, Methodology. **Xiaodan Xu:** Conceptualization, Data curation. **Xiaogang He:** Writing – original draft. **Ying Wang:** Methodology. **Yetian Li:** Resources. **Feifei Li:** Conceptualization, Funding acquisition, Supervision, Validation, Writing – review & editing, Resources, Visualization.

Declaration of competing interest

The authors declare that they have no competing interests.

Ethics approval and consent to participate

The study was performed with the approval of the Ethics Committee of the Experimental Animal Ethics Committee of Anhui Medical University (Approval NO.: LLSC20210808).

Consent for publication

All authors read and approved the submission and final publication.

Data availability

Data are available from the authors upon reasonable request.

Funding

This work was supported by the National Natural Science Foundation of China (Nos. 82173377, 81302319), the Major Research Project of Education Department of Anhui Province (KJ2018ZD018).

Supplementary materials

Supplementary material associated with this article can be found, in the online version, at [doi:10.1016/j.neo.2024.100967](https://doi.org/10.1016/j.neo.2024.100967).

References

- [1] R.L. Siegel, et al., Cancer statistics, CA. Cancer J. Clin 73 (1) (2023) 17–48.
- [2] F. Derakhshan, et al., Pathogenesis of triple-negative breast cancer, Annu. Rev. Pathol 17 (2022) 181–204.
- [3] Y. Hassaine, et al., Evolution of breast cancer incidence in young women in a French registry from 1990 to 2018: towards a change in screening strategy? Breast. Cancer. Res 24 (1) (2022) 87.
- [4] E.A. Mittendorf, et al., Neoadjuvant atezolizumab in combination with sequential nab-paclitaxel and anthracycline-based chemotherapy versus placebo and chemotherapy in patients with early-stage triple-negative breast cancer (IMpassion031): a randomised, double-blind, phase. 3. trial.. *Lancet* 396 (10257) (2020) 1090–1100.
- [5] P. Ferrari, et al., Molecular mechanisms, biomarkers and emerging therapies for chemotherapy resistant TNBC, Int. J. Mol. Sci 23 (3) (2022).
- [6] A. Dongre, et al., New insights into the mechanisms of epithelial-mesenchymal transition and implications for cancer, Nat. Rev. Mol. Cell. Biol 20 (2) (2019) 69–84.
- [7] T. Guan, et al., Phosphorylation of USP29 by CDK1 governs TWIST1 stability and oncogenic functions, Adv. Sci. (Weinh) 10 (11) (2023) e2205873.
- [8] S. Li, et al., BOP1 confers chemoresistance of triple-negative breast cancer by promoting CBP-mediated beta-catenin acetylation, J. Pathol 254 (3) (2021) 265–278.
- [9] K.S. Jeng, et al., Cellular and molecular biology of cancer stem cells of hepatocellular carcinoma, Int. J. Mol. Sci 24 (2) (2023).
- [10] J.N. Zhou, et al., A functional screening identifies a new organic selenium compound targeting cancer stem cells: role of c-Myc transcription activity inhibition in liver cancer, Adv. Sci. (Weinh) 9 (22) (2022) e2201166.
- [11] Y. Katsuno, et al., Chronic TGF-beta exposure drives stabilized EMT, tumor stemness, and cancer drug resistance with vulnerability to bitopic mTOR inhibition, Sci. Signal 12 (570) (2019).
- [12] A. Sulaiman, et al., Clinically translatable approaches of inhibiting TGF-beta to target cancer stem cells in TNBC, Biomedicine 9 (10) (2021).
- [13] X.Q. Li, et al., Extracellular vesicle-packaged CDH11 and ITGA5 induce the premetastatic niche for bone colonization of breast cancer cells, Cancer. Res 82 (8) (2022) 1560–1574.
- [14] X. Yin, et al., RUNX2 recruits the NuRD(MTA1)/CRL4B complex to promote breast cancer progression and bone metastasis, Cell. Death. Differ 29 (11) (2022) 2203–2217.
- [15] T.C. Lin, RUNX2 and cancer, Int. J. Mol. Sci 24 (8) (2023).
- [16] C. Zhang, et al., Runx2 deficiency in osteoblasts promotes myeloma resistance to bortezomib by increasing TSP-1-dependent TGFbeta1 activation and suppressing immunity in bone marrow, Mol. Cancer. Ther 21 (2) (2022) 347–358.
- [17] R. Kanwal, et al., Acquisition of tumorigenic potential and therapeutic resistance in CD133+ subpopulation of prostate cancer cells exhibiting stem-cell like characteristics, Cancer. Lett 430 (2018) 25–33.
- [18] X. Xu, et al., TGF-beta plays a vital role in triple-negative breast cancer (TNBC) drug-resistance through regulating stemness, EMT and apoptosis, Biochem. Biophys. Res. Commun 502 (1) (2018) 160–165.
- [19] L. Zhang, et al., MSX2 initiates and accelerates mesenchymal stem/stromal cell specification of hPSCs by regulating TWIST1 and PRAME, Stem. Cell. Reports 11 (2) (2018) 497–513.
- [20] J. Li, et al., Adjuvant capecitabine with docetaxel and cyclophosphamide plus epirubicin for triple-negative breast cancer (CBCSG010): an open-label, randomized, multicenter, phase III trial, J. Clin. Oncol 38 (16) (2020) 1774–1784.
- [21] G.K. Gupta, et al., Perspectives on triple-negative breast cancer: current treatment strategies, unmet needs, and potential targets for future therapies, Cancers. (Basel) 12 (9) (2020).
- [22] H. Feng, et al., Leptin acts on mesenchymal stem cells to promote chemoresistance in osteosarcoma cells, Aging. (Albany. NY) 12 (7) (2020) 6340–6351.
- [23] M. Futakuchi, et al., The effects of TGF-beta signaling on cancer cells and cancer stem cells in the bone microenvironment, Int. J. Mol. Sci 20 (20) (2019).
- [24] J.V. Joseph, et al., TGF-beta promotes microtubule formation in glioblastoma through thrombospondin 1, Neuro. Oncol 24 (4) (2022) 541–553.
- [25] C. Wang, et al., CBFbeta promotes colorectal cancer progression through transcriptionally activating OPN, FAM129A, and UPP1 in a RUNX2-dependent manner, Cell Death Differ 28 (11) (2021) 3176–3192.
- [26] B. Kim, et al., A CTGF-RUNX2-RANKL axis in breast and prostate cancer cells promotes tumor progression in bone, J. Bone. Miner. Res 35 (1) (2020) 155–166.
- [27] J.H. Park, et al., Nuclear IL-33/SMAD signaling axis promotes cancer development in chronic inflammation, EMBO. J 40 (7) (2021) e106151.
- [28] W. Si, et al., RUNX2 facilitates aggressiveness and chemoresistance of triple negative breast cancer cells via activating MMP1, Front. Oncol 12 (2022) 996080.
- [29] L. Zhang, et al., miR-205/RunX2 axis negatively regulates CD44(+)/CD24(-) breast cancer stem cell activity, Am. J. Cancer. Res 10 (6) (2020) 1871–1887.
- [30] P. Zhang, et al., Runx2 is required for activity of CD44(+)/CD24(-/low) breast cancer stem cell in breast cancer development, Am. J. Transl. Res 12 (5) (2020) 2305–2318.